LUT University

Simulation Model to Investigate Effect of Support Stiffness on Dynamic Behaviour of a Large Rotor

Kurvinen Emil, Viitala Risto, Choudhury Tuhin, Sopanen Jussi

This is a Author's accepted manuscript (AAM) version of a publication

published by CRC Press/Balkerna

in 12th International Conference on Vibrations in Rotating Machinery (VIRM)

DOI: 10.1201/9781003132639-37

Copyright of the original publication: © 2020 Taylor & Francis Group, London, UK

Please cite the publication as follows:

Kurvinen, E., Viitala, R., Choudhury, T., Sopanen, J. (2020). Simulation Model to Investigate Effect of Support Stiffness on Dynamic Behaviour of a Large Rotor. 12th International Conference on Vibrations in Rotating Machinery (VIRM). CRC Press/Balkerna. DOI: 10.1201/9781003132639-37

This is an Accepted Manuscript of a book chapter published by CRC Press in 12th International Conference on Vibrations in Rotating Machinery (VIRM) on 23.10.2020, available online: https://www.taylorfrancis.com/books/e/9781003132639

This is a parallel published version of an original publication. This version can differ from the original published article.

Simulation Model to Investigate Effect of Support Stiffness on Dynamic Behaviour of a Large Rotor

E. Kurvinen[1)], **R. Viitala**[2)], **T. Choudhury**[1)] **and J. Sopanen**[1)]

[1)] LUT University, Department of Mechanical Engineering, Finland
[2)] Aalto University, Department of Mechanical Engineering, Finland

ABSTRACT

In this study, the effect of support stiffness on the dynamic behaviour of a large industrial rotor is studied using simulation models and experimental test setup having a mechanical apparatus for changing the horizontal support stiffness. Two different simulation models with different levels of complexity were created to simulate the behaviour of the system. Such verified simulation models can be used to predict the critical speeds and minimum vibration operating speed areas. The achievements of this paper could be utilized in the industries using large rotors when operating conditions can be taken into consideration already in rotor system development.

1. INTRODUCTION

In rotating machinery, supports have a critical role as they affect the critical speeds of the system, e.g. in turbomachinery industry (1, 2) and power industry (3). Similarly, in the paper and steel industries, the supports have a significant effect on the dynamic behaviour of relatively large rotors, as subcritical frequencies are on the operational speed range and there are several sources of excitations due to the manufacturing inaccuracies, e.g. non-circular bearing geometries. To avoid these critical frequencies, one approach is to adjust the support stiffness and minimize the operational responses in the paper and steel industry applications.

The large rotors for paper and steel industries are typically made by bulk manufacturing process with very limited customization possibilities. However, rotors manufactured in the same production line can have a significant variation in their dynamic behaviour. This is related to the inaccuracies of manufacturing process that cause e.g. the thickness variation in a rotor body. In large rotating machines, the critical speeds are naturally low which increase the requirements of supporting structure; the supports of large machines need to be massive and highly stiff to preserve high enough critical speeds. Otherwise, the critical speed or its subcritical frequencies decrease, and resonances are possible.

To gain a deeper understanding of the root causes of the dynamic behaviour of a manufactured rotor a physics based white-box model together with measurements can be utilized (4). Nevertheless, the functionality of a rotor is not guaranteed even if the rotor is perfectly manufactured; the operational conditions of a rotor has a remarkable effect on rotor behaviour. Therefore, dynamic rotor behaviour could be only estimated, since the eventual effect of the operating conditions of the rotating system are unknown. The idea of manufacturing for the operating conditions is

discussed earlier in several publications where the rotors are optimized to correspond to the demands of the final installation location. For example, Kuosmanen (5) and Widmaier (6) have proven that the dynamic run-out of a rotor could be decreased when the operating conditions were taken into account. In (5) and (6), the rotor feedback measurement was conducted in operating conditions and then with 3D grinding, the dynamic run-out caused by the thickness variation and thermal run-out were compensated. A simulation model for a large rotor was created by Sopanen et al. (7) using flexible multibody formulation along with nonlinear bearing model. Heikkinen et al. (7) proposed a model based on Timoshenko beam elements including the effect of nonlinear bearings with asymmetric rotor properties. They studied the waviness of bearing inner ring and showed that it has significant effect on the dynamic run-out. Viitala et al. (8) developed a predictive method that minimize the excitation from bearing inner ring waviness. In their research, the roundness error of bearing inner ring were reduced by the compensative grinding of the bearing surface.

In this paper, a novel simulation application is presented that focuses on the simulation of the behaviour of a rotor under different speeds and support stiffnesses. The objective of this paper is to study the operational speed map (OSP). The OSP defines the operation speed range and support stiffness values and response amplitudes. These are studied by using two simulation models having different levels of complexity. The first one is a simplified three degree of freedom model that includes the rotor, the supports and the bearings with waviness excitation. Second model is a high-fidelity model proposed by Heikkinen et al. (7). In this paper, the model proposed in (7) is further developed for computational efficiency and parallel computing is utilized to calculate transient behaviour under different speeds and support stiffnesses. The model based on Timoshenko beam elements and nonlinear spherical roller bearings proposed by (9) is computationally efficient, which allows to study the operational speed map for given bearing excitations at various support stiffness and speed conditions in matter of hours. In the actual experimental setup, even if an adjustable stiffness device is available, the measurement process takes a week due to time consumed in changing the support stiffness and speed and capturing the steady state response. Operational speed maps obtained using simulation models are compared with the measured OSP. With the developed simulation method, the effects of support stiffness on the rotor behaviour can be predicted and by using the yielded information, the rotor and support design can be optimized.

The simulation model can be used as a virtual sensor to determine the support stiffness and thus additional stiffness measurement in the current system can be avoided. This can be accomplished as the response peaks that are visible at subharmonic frequencies, e.g. from the acceleration measurements, can be compared to the operational speed map. The virtual sensor can be used to identify the system on the field, which in turn would help in optimizing the dynamic behaviour. In addition, the simulation model can aid in designing the rotor, as in early design phase, the operational speed map can be studied and thus, optimal stiffness values and operational speeds can be selected. As one additional possibility for already manufactured large rotor systems, the support stiffness properties can be identified, and then either stiffened or loosened by adding or removing material from the supports for optimal dynamic behaviour for the application.

2. ROTORDYNAMICS, SIMULATION MODELS AND CASE STUDY

2.1 Rotordynamics

The test rotor used in this study has been considered as a flexible rotor. This means that the test rotor is assumed to have flexural modes. The determination affects specially to the balancing of a rotor, since the flexible rotors have practically infinite

number of bending modes with their own critical speeds. However, a significant impact is typically only in the first modes. A rotor can be modelled and balanced also as a rigid rotor, if flexural modes are not remarkable. ISO 21940-12 (10) gives guidance for the determination of a correct rotor type in relation to an operation speed. In there a rotor can be considered rigid if the first flexural resonance speed exceeds the maximum service speed by at least 50 %.

Subharmonic frequencies are integer fractions of the critical speeds. Those occur at 1/2, 1/3, 1/4, …, etc. times a critical speed. Subharmonic frequencies are harmful for large rotating machines that usually uses the frequencies under the critical speed. At these frequencies, harmonic excitation causes resonance in which the excitation frequency coincidence with the critical speed. The harmonic excitation produces the excitation as a function of rotating speed. Typical source for the harmonic excitation can be e.g. the thickness variation of a rotor body that produces excitation two times per revolution. This kind of excitation causes the resonance at speed of 1/2 times the critical speed and, thus, this speed is also called as half critical speed. Similar mechanism excites also lower subharmonic frequencies.

2.2 Simulation model descriptions

Two simulation models with different levels of complexity are utilized in this study. The first one (simple) is a three degree of freedom model that can describe the first flexible mode of a rotor-bearing-support system. The second model (detailed) is a beam element model of the rotor including rotor's asymmetry due the shell thickness variation as well as nonlinear spherical roller bearing model. Both simulation models include description of bearing waviness excitation. The simplified model is solved in frequency domain while the detailed model is solved with time transient numerical integration.

2.2.1 Three degree of freedom model (simple)

The three degree of freedom model is constructed in such a way that it can represent the first flexible mode of the roll-support system. Since the first flexible mode is symmetric, the model represents only one half of the actual system. Supported roll and free-free roll behaviour is depicted in Figure 1.

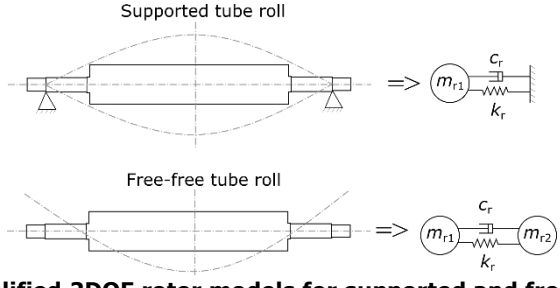

Figure 1. Simplified 2DOF rotor models for supported and free-free rotor.

The supported rotor's critical frequency (f_{supp}) and free-free frequency (f_{free}) can calculated as

$$f_{\text{supp}} = \frac{1}{2\pi}\sqrt{\frac{k_r}{m_{r1}}} \qquad (1) \qquad f_{free} = \frac{1}{2\pi}\sqrt{\frac{k_r\left(m_{r1}+m_{r2}\right)}{m_{r1}m_{r2}}}\,, \qquad (2)$$

where k_r is the support stiffness, m_{r1} represents the middle part of the rotor and m_{r2}, represents the end part of the rotor.

Figure 2 shows the schematic of the model. In the model, one half of the roll is further divided into two parts (m_{r1} and m_{r2}) that are connected with spring (k_r) and damper (c_r). The roll is connected to support (m_s) with bearings having spring coefficient (k_b) and damping coefficient (c_b), while the support mass (m_s) is connected with spring (k_s) and damper (c_s) to the ground.

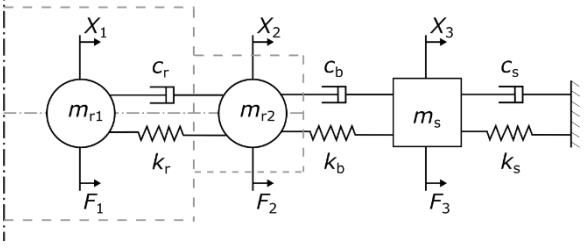

Figure 2. Schematic of simplified model of 3 DOF representing half of the rotor and one support.

To capture the first natural frequency of the roll properly with the simplified model, the following relations can be created:

1.) One-half of total mass of the roll is $m/2 = m_r = m_{r1} + m_{r2}$
2.) Supported roll frequency, f_{supp} = 30 Hz
3.) 1st free-free frequency of the roll, f_{free} =75 Hz

Using the above relations and Eqs. (1) and (2), the parameters for the simplified roll model can be obtained. The damping coefficient for the roll part (c_r) can be obtained by assuming 1% modal damping ratio. Support mass, m_s, is 190 kg. The bearing stiffness in horizontal direction is $2.5 \cdot 10^8$ N/m and the bearing damping (c_b) is assumed to be 0.25% of the bearing stiffness. The support stiffness is $2 \cdot 10^8$ N/m in vertical direction and in horizontal direction, it is varied from 2.14 MN/m to 18.34 MN/m. For support damping, c_s, 2% damping ratio to the critical damping coefficient is used.

Bearing inner ring waviness is assumed to cause harmonic excitation forces that are included in F_2 and F_3. Bearing waviness excitation mechanism is fairly complicated, but in this study, it is assumed to cause forced displacement excitation between the roll and support. In general, bearing waviness generates several harmonic excitations and the k^{th} harmonic waviness excitation can be written as

$$\delta_k = A_k \cos\left(k\omega t + \phi_k\right), \tag{3}$$

where A_k the amplitude and ϕ_k is the phase of the k^{th} is the order waviness, ω is the rotor rotating frequency. Waviness can be considered base motion, in which the excitation forces are transferred through the bearing stiffness and damping. Therefore, harmonic spring and damping forces for the k^{th} order waviness excitation can be written as follows

$$\begin{aligned} F_2(t) = &\underbrace{\left(-k_b A_k \sin\phi_k - c_b A_k k\omega \cos\phi_k\right)}_{F_s} \sin\left(k\omega t\right) + \\ &\underbrace{\left(k_b A_k \cos\phi_k - c_b A_k k\omega \sin\phi_k\right)}_{F_c} \cos\left(k\omega t\right) \end{aligned} \tag{4}$$

Corresponding counteraction force is applied to the support (F_3). Considering multiple waviness excitations, the equation of motion of system can be written as

$$\mathbf{M}\ddot{\mathbf{x}}(t)+\mathbf{C}\dot{\mathbf{x}}(t)+\mathbf{K}\mathbf{x}(t)=\sum_{k}\left(\mathbf{F}_{s}^{k}\sin k\omega t+\mathbf{F}_{c}^{k}\cos k\omega t\right) \quad (5)$$

Superposition principle can be used to obtain the final steady state solution as follows

$$\mathbf{x}(t)=\sum_{k}\left(\mathbf{a}^{k}\sin k\omega t+\mathbf{b}^{k}\cos k\omega t\right) \quad (6)$$

where the coefficient vectors $\mathbf{a}^{k}$ and $\mathbf{b}^{k}$ can be solved for each harmonic excitation *k* as follows

$$\begin{bmatrix}\mathbf{a}^{k}\\ \mathbf{b}^{k}\end{bmatrix}=\begin{bmatrix}\mathbf{K}-(k\omega)^{2}\mathbf{M} & -k\omega\mathbf{C}\\ k\omega\mathbf{C} & \mathbf{K}-(k\omega)^{2}\mathbf{M}\end{bmatrix}^{-1}\begin{bmatrix}\mathbf{F}_{s}^{k}\\ \mathbf{F}_{c}^{k}\end{bmatrix}. \quad (7)$$

2.2.2 High-fidelity simulation model (detailed)

In this section, the model developed by Heikkinen et al. (7) is implemented to the test case. The simulation model included asymmetric 3D beam elements based on Timoshenko beam theory. The asymmetry is induced by varying the thickness of the tube section based on ultrasonic measurement similarly as in (11). The thickness variation is implemented in the model by defining the thickness profiles of the cross sections along the length of the tube section, thus affecting to the area moment of inertia.

The rotor is supported with two SKF 23124 CCK/W33 spherical roller bearings. The spherical roller bearings are modelled with nonlinearity included, similarly as in Ghalamchi et al. (9). In the simulations the nominal bearing clearance of 60 µm is used, and measured waviness profiles of measured sections are shown in Table 1. Waviness components from twice to six times per revolution were measured from the bearing inner ring for the service end and drive end of the machine.

Table 1. Measured bearing inner ring roller path waviness amplitudes.

Service end	First roller element path			Second roller element path		
	k	Amplitude [µm]	Phase [rad]	*k*	Amplitude [µm]	Phase [rad]
	2	0.4647	7.1075	2	0.5757	5.5588
	3	0.1501	1.6304	3	0.1304	7.5205
	4	0.2520	2.8345	4	0.2024	2.8113
	5	0.3197	4.0324	5	0.4019	3.8472
	6	0.1475	1.8118	6	0.0479	3.7840
Drive end						
	2	0.4361	2.9981	2	0.4802	7.6331
	3	0.4186	3.6507	3	0.4092	3.6553
	4	0.3121	7.7142	4	0.1651	7.4677
	5	0.3346	2.5530	5	0.1176	1.6024
	6	0.1569	5.1329	6	0.1283	4.2674

The measured roll section thickness variations are included in the simulation model. The supports are modelled as mass-spring-damper elements, individually in horizontal and vertical directions. Damping for support structures has 2% damping ratio for horizontal and 3% for vertical direction. Modal damping ratios 1.5% (1st), 2% (2nd), 2.5% (3rd) and 3.0% (4th to 6th) where the value in parenthesis corresponds to the flexible mode number. In the transient analysis, model reduction is applied and the number of retained modes is 16. Simulation runs are conducted for 9 seconds with a sampling rate of 2000 Hz (time-step of 0.0005s). The resulting response are captured at the bearing locations. The computational time is approximately 300 seconds per single simulation of 9 seconds. However, the computation time is dependent on the system parameters, such as parameters of nonlinear bearing model. Calculations are conducted with a Triton cluster (Node Dell PowerEdge C6420 with 2x20 core Xeon Gold 6148 at 2.4 GHz and 192 GB DDR4-2667 memory), having

two nodes, both with 40 CPU's parallel computing. With that setup, the computation time is 15 hours.

2.3 System and measurement setup

The test setup has a possibility to vary the horizontal stiffness and thus, similar data set could be measured as generated in the simulation. The adjustable stiffness in the test setup is implemented by using a similar structure as in balancing machines where a rotor is supported by plate springs. Subsequently, the stiffness for the support is provided through an external beam. The structure is implemented at both rotor ends. The mechanism for adjustable stiffness and force sensor locations are depicted in Figure 3.

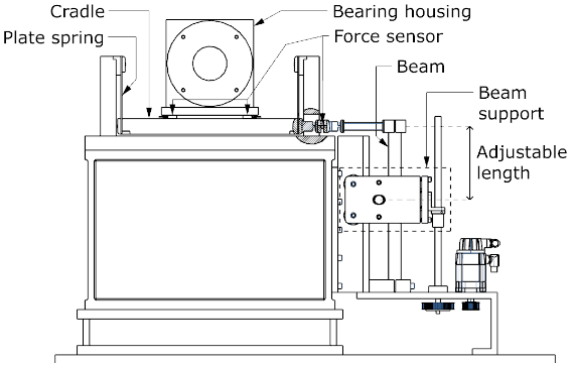

Figure 3. Mechanism for adjusting the support stiffness in horizontal direction.

The studied rotor is a paper machine guiding roll (tube roll). The mass of the rotor is 720 kg with a total length of 5 m and a 4 m long tube section. Figure 4 shows the significant dimensions of the rotor. Other additional masses that affect to the horizontal movement of the shaft ends are the bearing housing masses and the masses of the parts that constitute the adjustable stiffness device (m_s).

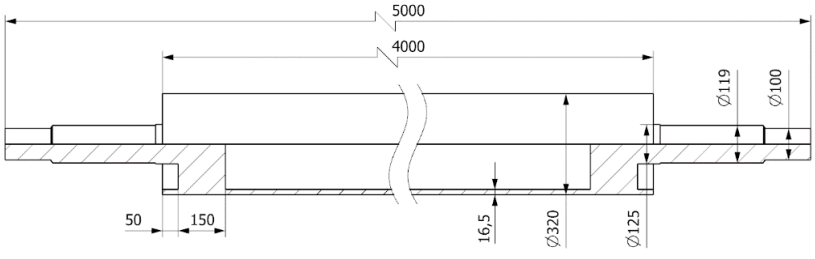

Figure 4. Studied rotor cross-section with dimensions (in mm).

The verification measurement is conducted by using the radial bearing force sensors at both bearings. The measured rotation speed range is 4 – 18 Hz in which the rotor is accelerated with 0.05 Hz increments. The acceleration ramp is repeated with 31 different stiffnesses. The acceleration is limited to the maximum speed below the critical speed. The measurement procedure is conducted as follows:

1. The stiffness is adjusted at the lowest point
2. The rotor is accelerated at 4 Hz
3. 100 rounds are measured

4. The rotor speed is increased with the increment of 0.05 Hz
5. Steps 4 and 5 are repeated until the last rotating speed is reached
6. The stiffness is increased
7. Steps 2 to 6 are repeated until the last stiffness level is reached.

The measured data is post processed using time synchronous averaging (TSA) that is originally developed by (12, 13) The method enables the averaging of a phase locked signal and representing it as a single round. From this averaged signal the maximum values of each direction (horizontal and vertical) are captured. The details of the force measurement setup can be found in Viitala's et al. (14) research in which same measurement method was used.

3. RESULTS

3.1 Simulation model and validation

The simulation models are validated with free-free frequencies and supported frequencies measured from actual machine, i.e. 75 Hz for free-free rotor, and supported frequencies of 20.9 Hz in horizontal direction and 30 Hz in vertical direction. The first and second bending modes (horizontal) of the rotor are shown in Figure 5. In the vertical direction, the first bending mode occurs at 30 Hz (30.5 Hz with infinitely stiff support).

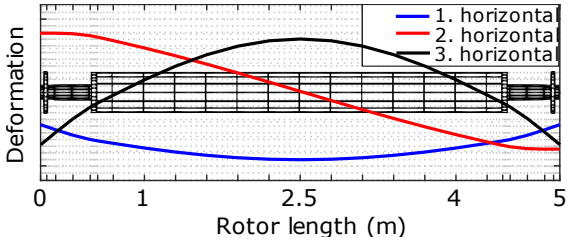

Figure *5.* First and second horizontal bending modes at 20.9 Hz and 34.3 Hz with maximum support stiffness.

3.1.1 Operational speed map with simple simulation model

Figure 6 depicts the simple simulation response results. In the model, the waviness amplitudes of the service end at the first roller path are used. Due to the computational simplicity of the model, the results are calculated with 100 different stiffness values and speed range from 0 to 18 Hz. The numbering e.g. "1-2" refers to 1st bending mode and 2nd fraction of critical speed etc.

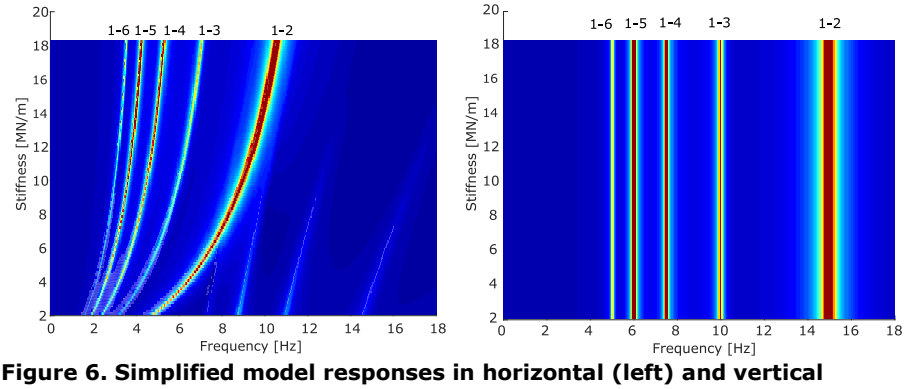

Figure 6. Simplified model responses in horizontal (left) and vertical (right) directions.

3.1.2 Operational speed map with detailed simulation model

In the analysis, 281 points from 4 Hz to 18 Hz (increment of 0.05 Hz) are analysed along with 31 different horizontal support stiffness values, yielding to a network of 8711 calculations. From these simulations, the maximum amplitude is captured and plotted with the speed and stiffness values used in the analysis. Figure 7 depicts the operation speed map for horizontal and vertical directions.

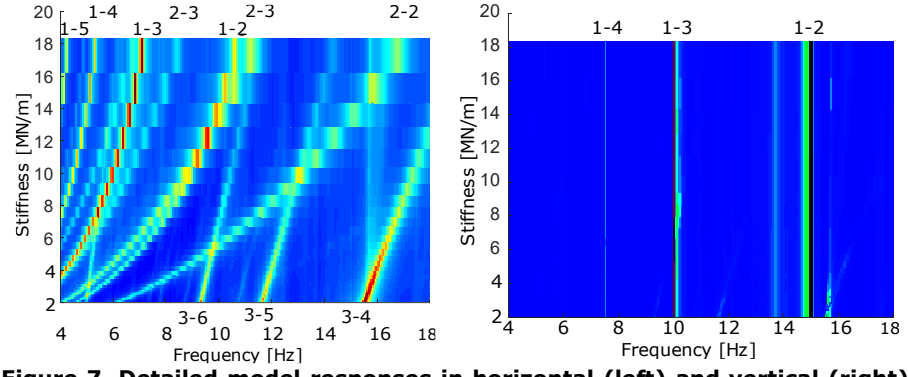

Figure 7. Detailed model responses in horizontal (left) and vertical (right) directions.

3.1.3 Operational speed map with measurement

In the measurement, with the highest stiffness value set in the horizontal direction, the full range of 4 Hz to 18 Hz with 0.05 Hz increments is measured. As the support stiffness is decreased the maximum speed is decreased to avoid resonance with the 1x component in the measurements.

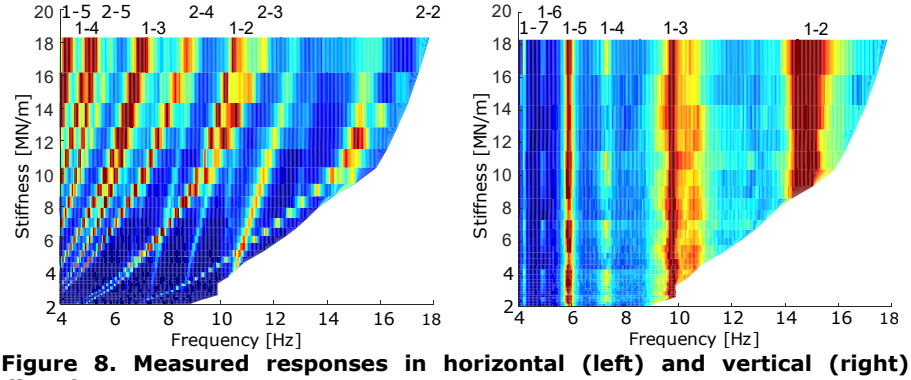

Figure 8. Measured responses in horizontal (left) and vertical (right) directions.

3.2 Results comparison

Table 2 depicts the results comparison at the highest stiffness 18.32 MN/m and at the lowest stiffness 2.04 MN/m. In the table the frequency peaks shown in Figure 6-Figure 8 are collected and compared.

Table 2. Comparison of simulated and measured horizontal subharmonic frequencies

Support stiffness (MN/m)	Mode # - harmonic	Simulated (Simple) (Hz)	Simulated (Detailed) (Hz)	Measured (Hz)	Difference measured to simple [%]	Difference measured to detailed [%]
18.32	1-2	10.60	10.60	10.58	0.19	0.19
	1-3	7.05	7.05	7.06	-0.14	-0.14
	1-4	5.30	5.35	5.32	-0.38	0.56
	1-5	4.25	4.25	4.27	-0.47	-0.47
	2-2	-	16.80	17.84	-	-6.19
	2-3	-	11.20	11.63	-	-3.84
	2-4	-	8.45	8.75	-	-3.55
	3-5	-	14.40	12.82	-	10.97
	3-6	-	11.60	10.83	-	6.64
	3-7	-	-	9.15	-	-
	3-8	-	-	8.05	-	-
2.04	1-2	4.80	4.65	4.97	-3.44	-3.44
	2-2	-	6.25	6.90	-	-10.46
	2-3	-	4.15	4.62	-	-11.25
	3-4	-	15.55	-	-	-
	3-5	-	11.65	-	-	-
	3-6	-	9.25	8.49	-	8.22
	3-7	-	-	7.20	-	-
	3-8	-	-	6.31	-	-

4. DISCUSSION

A comparison between the simplified and detailed simulation models shows that the accuracy is almost same for both models when considering the 1st bending mode. Both agree well with the measurements and have less than 1% error compared to measured results in case of the highest support stiffness and, correspondingly, 3.5% error in case of the lowest support stiffness. The simplified simulation model only consists of the first bending mode and thus is not able to show higher modes.

With 2nd bending mode, the detailed simulation model gives approximately 4-6% lower frequencies compared to measured ones at the highest support stiffness and 11% lower frequencies in case of the lowest support stiffness. For the 3rd bending mode, the detailed simulation model estimates 6-10% higher frequencies than measured at the highest support stiffness and 8% higher frequency in case of the lowest support stiffness. With lowest support stiffness the support behaviour becomes more dominant when compared to the highest stiffness where the rotor flexibility is more dominating. The higher order waviness components are visible well in both simulation models.

As can be interpreted from the results, variation of the horizontal support stiffness affects differently to different bending critical frequencies of the modes. In simulation results of both models, the relative frequency change is remarkably similar as in the verification measurements. In the measurements, the support stiffness was lowered 88.9% from its highest value and this yielded 53.6%, 60.7% and 21.1% change in the first, second and third measured bending mode frequencies, respectively. This result reveals the sensitivity of each bending critical speed to the variation of support stiffness. The corresponding changes in the detailed simulation were 56.1%, 62.8%, 19.1%. Thus, the largest relative error 2.5% was in the first mode. The simple simulation model yielded 54.4% change in the first mode frequency that is even closer than the relative change in detailed simulation model.

Finally, it should be noted that the 7th and 8th harmonic response due to bearing waviness can be seen in the measurements but those are not included in the simulations. However, from practical point of view the higher order waviness components does not have significant role.

5. CONCLUSIONS

The two simulation models were created and their capacity of producing operational speed map in a case study were reported. The study shows that the simple model can reproduce the operational speed map within 0.5% accuracy when compared to measured operational speed map. However, this model can describe only the first flexible bending mode. Furthermore, when the simple and complex simulation cases were compared, there was no major difference in the results to the first bending mode, i.e. the asymmetry and nonlinearity is not causing major effect to the results. The addition that the detailed model gives is the inclusion of second and third bending mode and their effect is visible in the operational speed map. To summarize, the simple model can generate operational speed map with a high accuracy and from computationally point of view, the calculation can be made within seconds, even with very fine computational grid. To design the large rotors for specific application, such maps helps to optimize the application specific rotation speed to designed support stiffness value.

Aknowledgement

The research was funded by the Academy of Finland (project no. 313675 and 313676). We acknowledge the computational resources provided by the Aalto Science-IT project.

REFERENCES

[1] J. Hong, K. Shaposhnikov, D. Zhang, and Y. Ma, "Theoretical modeling for a rotor-bearing-foundation system and its dynamic characteristics analysis," in *Proceedings of the 9th IFToMM International Conference on Rotor Dynamics*. Springer, 2015, pp. 2199–2214.

[2] W. Yan, K. Shaposhnikov, P. Yu, Y. Ma, and J. Hong, "Experimental investigation and numerical analysis on influence of foundation excitation on the dynamics of the rotor system," in *ASME Turbo Expo 2015: Turbine Technical Conference and Exposition*. American Society of Mechanical Engineers Digital Collection, 2015.

[3] P. Paturu, I. Vinoth Kanna, and G. Mallela, "A detailed analysis of free vibration on 70 mw hydro power turbine rotor," *International Journal of Ambient Energy*, pp. 1–8, 2019.

[4] M. Cocconcelli, L. Capelli, J. Cavalaglio Camargo Molano, and D. Borghi, "Development of a methodology for condition-based maintenance in a large-scale application field," *Machines*, vol. 6, no. 2, p. 17, 2018.

[5] P. Kuosmanen, *Predictive 3D roll grinding method for reducing paper quality variations in coating machines*. Helsinki University of Technology, 2004.

[6] T. Widmaier, *Optimisation of the roll geometry for production conditions*. Aalto University Publication Series Doctoral Dissertations 156/2012. 184 p, 2012.

[7] J. E. Heikkinen, B. Ghalamchi, R. Viitala, J. Sopanen, J. Juhanko, A. Mikkola, and P. Kuosmanen, "Vibration analysis of paper machine's asymmetric tube roll supported by spherical roller bearings," *Mechanical Systems and Signal Processing*, vol. 104, pp. 688 – 704, 2018.

[8] R. Viitala, T. Widmaier, and P. Kuosmanen, "Subcritical vibrations of a large flexible rotor efficiently reduced by modifying the bearing inner ring roundness profile," *Mechanical Systems and Signal Processing*, vol. 110, pp. 42–58, 2018.

[9] B. Ghalamchi, J. Sopanen, and A. Mikkola, "Simple and versatile dynamic model of spherical roller bearing," *International Journal of Rotating Machinery*, vol. 2013, 2013.

[10] "ISO ISO21940-12 Mechanical vibration. Rotor balancing. Part 12: Procedures and tolerances for rotors with flexible behaviour," International Organization for Standardization, Geneva, CH, Standard, 2016.

[11] J. Juhanko, E. Porkka, T. Widmaier, and P. Kuosmanen, "Dynamic geometry of a rotating cylinder with shell thickness variation," *Estonian Journal of Engineering*, vol. 16, no. 4, p. 285, 2010.

[12] P. McFadden, "A revised model for the extraction of periodic waveforms by time domain averaging," *Mechanical Systems and Signal Processing*, vol. 1, no. 1, pp. 83–95, 1987.

[13] P. McFadden and M. Toozhy, "Application of synchronous averaging to vibration monitoring of rolling element bearings," *Mechanical Systems and Signal Processing*, vol. 14, no. 6, pp. 891–906, 2000.

[14] R. Viitala, R. Viitala, and P. Kuosmanen, "Method and device for large rotor bearing force measurement," in *2019 IEEE International Instrumentation and Measurement Technology Conference (I2MTC)*, May 2019, pp. 1–6.